



Detailed Anatomy of Bridging Veins Around the Foramen Magnum: a Multicenter Study Using Three-dimensional Angiography

Masafumi Hiramatsu¹ · Tomohiko Ozaki² · Shuichi Tanoue³ · Katsuhiko Mizutani⁴ · Hajime Nakamura⁵ · Kohei Tokuyama⁶ · Hiroyuki Sakata⁷ · Yuji Matsumaru⁸ · Ichiro Nakahara⁹ · Yasunari Niimi¹⁰ · Toshiyuki Fujinaka² · Hiro Kiyosue¹¹

Received: 25 May 2023 / Accepted: 14 June 2023 / Published online: 8 August 2023
© The Author(s) 2023

Abstract

Background and Purpose There has been limited literature regarding the bridging veins (BVs) of the medulla oblongata around the foramen magnum (FM). The present study aims to analyze the normal angioarchitecture of the BVs around the FM using slab MIP images of three-dimensional (3D) angiography.

Methods We collected 3D angiography data of posterior fossa veins and analyzed the BVs around the FM using slab MIP images. We analyzed the course, outlet, and number of BVs around the FM. We also examined the detection rate and mean diameter of each BV.

Results Of 57 patients, 55 patients (96%) had any BV. The median number of BVs was two (range: 0–5). The BVs originate from the perimedullary veins and run anterolaterally to join the anterior condylar vein (ACV), inferior petrosal sinus, sigmoid sinus, or jugular bulb, inferolaterally to join the suboccipital cavernous sinus (SCS), laterally or posterolaterally to join the marginal sinus (MS), and posteriorly to join the MS or occipital sinus. We classified BVs into five subtypes according to the draining location: ACV, jugular foramen (JF), MS, SCS, and cerebellomedullary cistern (CMC). ACV, JF, MS, SCS, and CMC BVs were detected in 11 (19%), 18 (32%), 32 (56%), 20 (35%), and 16 (28%) patients, respectively. The mean diameter of the BVs other than CMC was 0.6 mm, and that of CMC BV was 0.8 mm.

Conclusion Using venous data from 3D angiography, we detected FM BVs in most cases, and the BVs were connected in various directions.

Keywords Bridging vein · Foramen magnum · Cone-beam CT · Venous phase three-dimensional rotational angiography · Slab maximum intensity projection · Dural arteriovenous fistula

✉ Masafumi Hiramatsu
mhiramatsu@okayama-u.ac.jp

¹ Department of Neurological Surgery, Okayama University Faculty of Medicine, Dentistry and Pharmaceutical Sciences, Okayama 700-8558, Japan

² Department of Neurosurgery, National Hospital Organization, Osaka National Hospital, Osaka, Japan

³ Department of Radiology, Kurume University School of Medicine, Kurume, Japan

⁴ Department of Neurosurgery, Keio University School of Medicine, Tokyo, Japan

⁵ Department of Neurosurgery, Osaka University Graduate School of Medicine, Osaka, Japan

⁶ Department of Radiology, Oita University Faculty of Medicine, Yuhu, Japan

⁷ Department of Neuroendovascular Therapy, Kohnan Hospital, Sendai, Japan

⁸ Division of Stroke Prevention and Treatment, Department of Neurosurgery, Faculty of Medicine, University of Tsukuba, Tsukuba, Japan

⁹ Department of Comprehensive Stroke, Fujita Health University School of Medicine, Toyoake, Japan

¹⁰ Department of Neuroendovascular Therapy, St Luke's International Hospital, Tokyo, Japan

¹¹ Department of Diagnostic Radiology, Kumamoto University Faculty of Medicine, Kumamoto, Japan

Abbreviations

3D-RA	Three-dimensional rotational angiography
ACV	Anterior condylar vein
BV	Bridging vein
CCJ	Cranio cervical junction
CE-CBCT	Contrast-enhanced cone-beam CT
CMC	Cerebellomedullary cistern
DAVF	Dural arteriovenous fistula
FM	Foramen magnum
IQR	Interquartile range
JF	Jugular foramen
MS	Marginal sinus
SCS	Suboccipital cavernous sinus
VA	Vertebral artery

Introduction

The bridging vein (BV) is a connecting vessel that drains venous blood flow from the brain's surface to the surrounding dural sinus. There are many BVs around the major dural sinuses, such as the superior sagittal and transverse sinuses. They have been analyzed in detail using various imaging modalities [1, 2]. Venous hypertension due to the dural arteriovenous fistula (dAVF) can cause venous reflux to the cerebral or cerebellar veins via the BVs, leading to venous congestion of the brain parenchyma and intracranial hemorrhage. The BVs of the medulla oblongata have crucial roles as the draining veins of specific dAVFs [3]. There has been limited literature on the BVs of the medulla oblongata around the foramen magnum (FM). Although there have been a few cadaveric studies of BVs around the FM, there has been no comprehensive research on angiographic anatomy. The present study aims to analyze the normal angioarchitecture of the BVs around the FM using slab MIP images of three-dimensional (3D) angiography.

Methods

All procedures performed in studies involving human participants were performed in accordance with the ethical standards of our institutional research committee. The institutional review boards approved this retrospective study in all collaborative institutions. Written informed consent was obtained from all patients before angiography; however, the need for informed consent for this study was waived because of the retrospective noninvasive study design. Participating centers were selected from among members of the Japanese Society for Neuroendovascular Therapy (JSNET) based on a recognized reputation for treating vascular disorders and an expressed interest in study participation.

Study Population

We included patients aged 20–80 years admitted to eight participating centers (Affiliation number 1–8) between January 2013 and October 2022 with 3D angiography data of posterior fossa veins. The 3D angiography data of posterior fossa veins included contrast-enhanced cone-beam CT (CE-CBCT) with long acquisition mode and venous phase 3D-rotational angiography (3D-RA) of the dominant side vertebral artery (VA). The CE-CBCT aimed to visualize micro-angioarchitecture such as implanted intracranial stent apposition or vertebral artery dissection. The aim of the venous phase 3D-RA was the preoperative evaluation of vascular disease or intracranial tumor and evaluation of venous disorder. We excluded patients with no venous 3D data of the region of interest, arteriovenous shunt disease, post-craniotomy of the posterior fossa, or insufficient data due to artifact or acquisition timing.

We collected the clinical and radiological data of 85 patients. Clinical characteristics were age, sex, and disease name. Radiological data were angiography in Digital Imaging and Communications in Medicine (DICOM) data format. Among them, 28 patients were excluded from this study based on the exclusion criteria described above: no venous 3D data of region of interest (21 patients), post-craniotomy (3 patients), and insufficient data for analyses (4 patients). The remaining 57 patients (31 males, 26 females; age range, 40–78 years; mean, 58 years) were retrospectively evaluated. All 57 patients had undergone 3D angiography of one-sided vertebral artery; thus, 57 3D data in total were analyzed. The underlying disease was an intracranial aneurysm in 35 patients, intracranial tumor in 12 patients, and other conditions such as suspected venous abnormality or pre-surgical evaluation of microvascular decompression in 10 patients.

Angiographic Evaluation

Diagnosis was carried out by members of this study group, a panel consisting of nine neurosurgeons and three neuroradiologists, all but one (K.T.) certified as neuro-interventionalists by the JSNET. All collected angiographic data were reviewed using Horos v.3.3.6, a free, open-source medical image viewer. The 3D data of posterior fossa veins were evaluated mainly using slab MIP images from CE-CBCT or venous phase 3D-RA. Because CE-CBCT with long acquisition mode included data on arteries and veins, we distinguished arteries and veins using CE-CBCT and arterial phase 3D-RA data (Fig. 1). We defined the BVs as including the radiculomedullary veins, which run along the cranial and spinal nerve roots. We analyzed the course, outlet, and number of BVs around the FM in each patient.

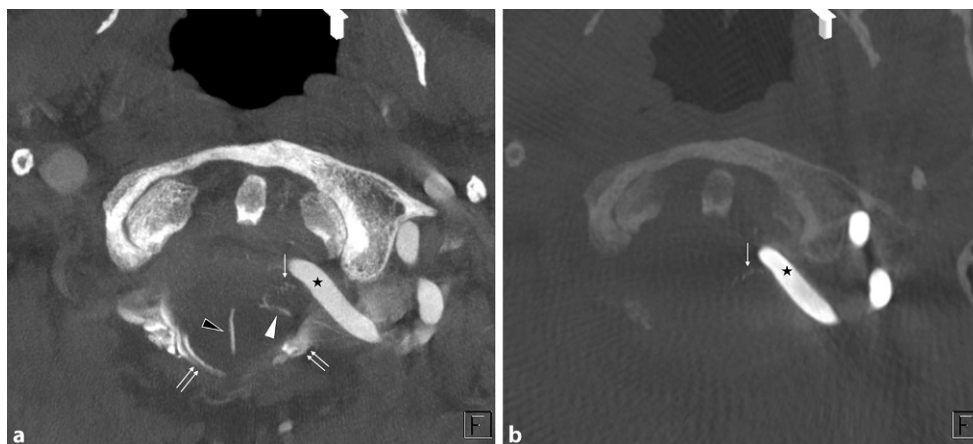


Fig. 1 Differentiation between arteries and veins in contrast-enhanced cone-beam CT (CE-CBCT). The axial view of the slab MIP images of CE-CBCT (**a**) and arterial phase three-dimensional rotational angiography (**b**). CE-CBCT with long acquisition mode includes data on arteries and veins. We can only observe arteries (*arrow*) in arterial phase three-dimensional rotational angiography (**b**). Consequently, we can confirm that the other vessels are veins (*white and black arrowheads*) or sinuses (*double arrows*) in CE-CBCT (**a**). *Star* shows the left vertebral artery

We also examined the detection rate and mean diameter of each BV.

Statistical Analyses

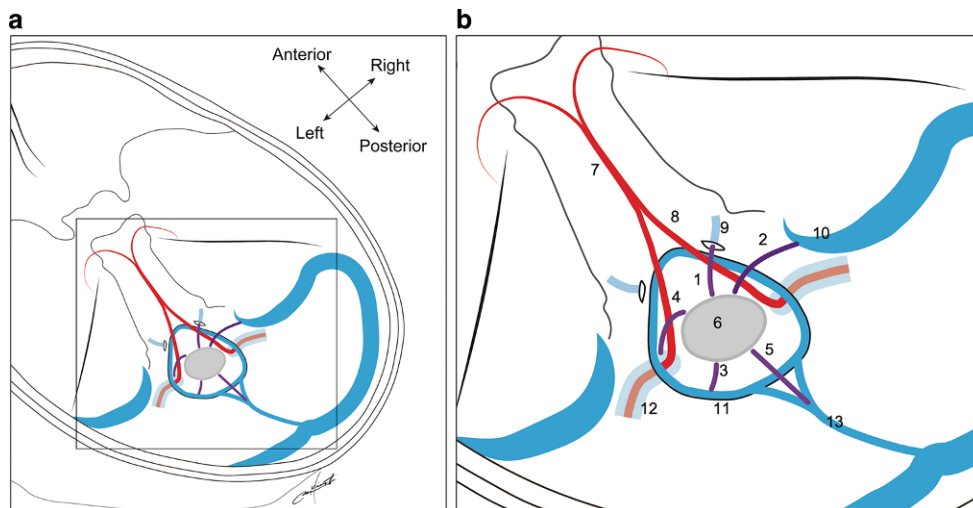
All calculations were performed using JMP 14 software (SAS Institute, Inc.). Radiological data, including angiographic modality, angiography side, and detection rate of BVs, were summarized using descriptive statistics. We described the number of detectable BVs as the median and interquartile range (IQR). The number of detectable BVs divided into angiography side (right and left) or imaging modality (CE-CBCT and 3D-RA) were assessed using the Wilcoxon signed-rank test. A p -value of 0.05 or lower was considered to be statistically significant. The diameter of each BV was described as mean and range.

Results

The baseline data of angiography were as follows: angiography side was right in 28 patients and left in 29 patients; imaging modality was CE-CBCT in 29 patients and venous phase 3D-RA in 28 patients.

Of 57 patients, 55 patients (96%) had any BV around the FM and a total of 122 BVs were detected. The number of BVs were 0, 1, 2, 3, 4, and 5 in 2, 16, 17, 17, 4, and 1 patients, respectively (median, 2 [IQR, 1–3]). We detected one to five BVs (median, 2 [IQR, 2–3]) in the 3D data of right-side VA angiography and zero to four BVs (median, 2 [IQR, 1–3]) in the 3D data of left-side VA angiography. There was no significant difference in the number of detected BVs according to the laterality of VA angiography ($p=0.23$). We detected zero to five BVs (median, 2 [IQR, 2–3]) in CE-CBCT data and one to four BVs (median, 2

Fig. 2 Schematic illustration (**a**) and its partly expanded illustration (**b**) of bridging veins (BVs) and surrounding vessels around the foramen magnum: 1 indicates the anterior condylar vein (ACV) BV; 2, jugular foramen (JF) BV; 3, marginal sinus (MS) BV; 4, suboccipital cavernous sinus (SCS) BV; 5, cerebello-medullary cistern (CMC) BV; 6, cross-section of the medulla oblongata; 7, basilar artery; 8, vertebral artery (VA); 9, ACV in the hypoglossal canal; 10, jugular bulb or sigmoid sinus; 11, MS; 12, SCS around the extracranial VA; 13, occipital sinus



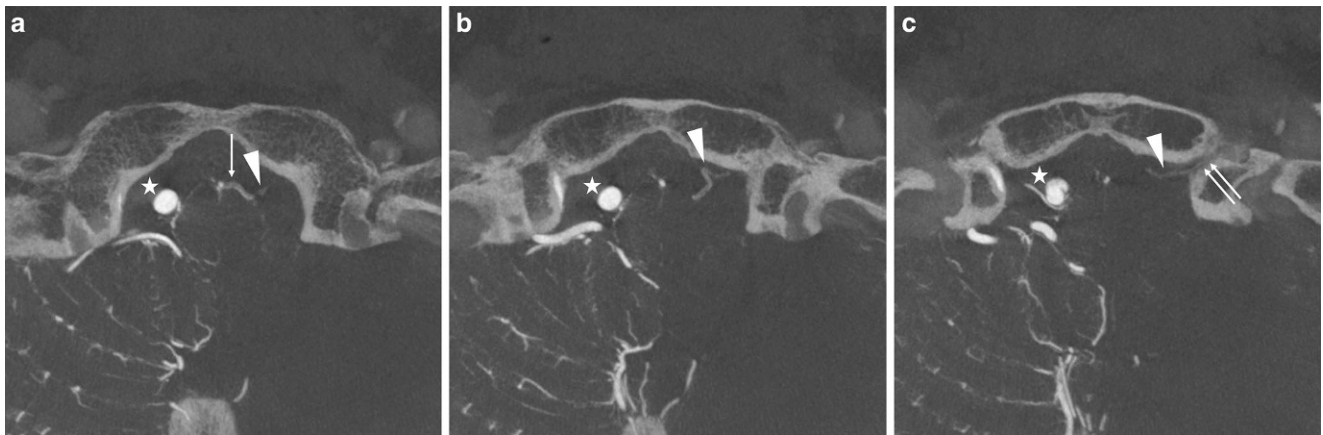


Fig. 3 A representative case of the anterior condylar vein (ACV) bridging vein (BV). Axial view of the slab MIP images from contrast-enhanced cone-beam CT shows that the transverse medullary vein (*arrow* in **(a)**) drains into the ACV (*double arrows* in **(c)**) in the hypoglossal canal via the ACV BV (*arrowheads* in **(a)**–**(c)**). *Star* shows the right vertebral artery

[IQR, 1–3]) in venous phase 3D-RA. There was no significant difference in the number of detected BVs according to the imaging modality ($p=0.13$).

Course and Terminations of BVs

The BVs originate from the perimedullary veins and run anterolaterally to join the anterior condylar vein (ACV),

inferior petrosal sinus, sigmoid sinus, or jugular bulb, inferolaterally to join the suboccipital cavernous sinus (SCS), laterally or posterolaterally to join the marginal sinus (MS), and posteriorly to join the MS or occipital sinus. We classified BVs around the FM into five subtypes based on the draining pattern into the surrounding venous sinus or vein (Fig. 2):

Fig. 4 A representative case of the jugular foramen (JF) bridging vein (BV). Axial (**a**) and coronal (**b**) view of the slab MIP images from contrast-enhanced cone-beam CT show that the transverse medullary vein (*arrow* in **(a)** and **(b)**) drains into the inferior petrosal sinus (*double arrows* in **(b)**) and sigmoid sinus (not shown) via two JF BVs (*white and black arrowheads*). *Star* shows the left vertebral artery running close to the opposite side

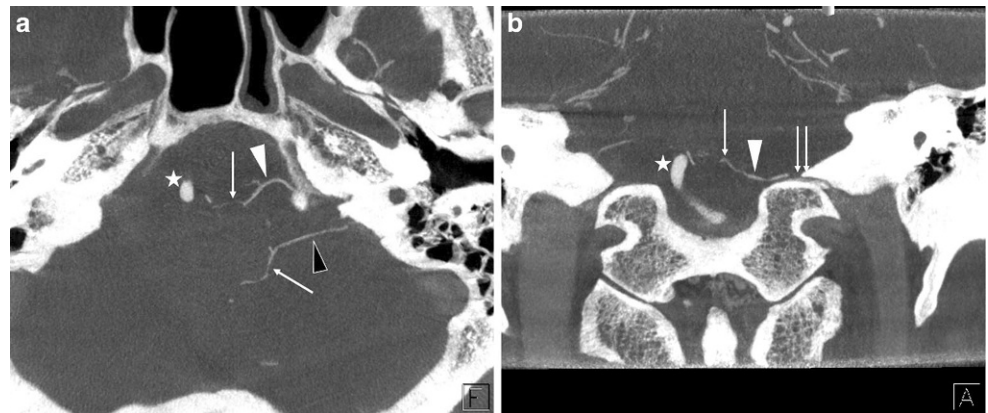


Fig. 5 A representative case of the marginal sinus (MS) bridging vein (BV). Axial (**a**) and coronal (**b**) view of the slab MIP images from contrast-enhanced cone-beam CT show that the transverse medullary vein (*arrow* in **(a)**) and lateral medullary vein (*arrow* in **(b)**) drains into the MS (*double arrows* in **(a)** and **(b)**) via two MS BVs (*white and black arrowheads*). *Star* shows the right vertebral artery

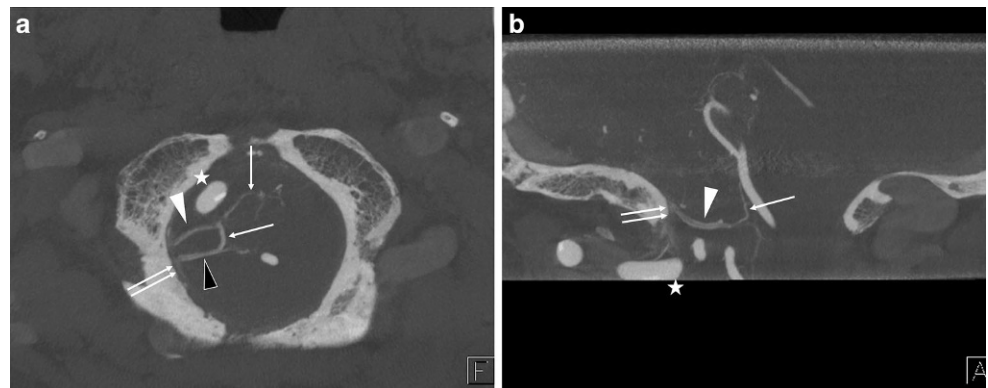


Fig. 6 A representative case of the suboccipital cavernous sinus (SCS) bridging vein (BV). Axial (a) and coronal (b) view of the slab MIP images from contrast-enhanced cone-beam CT show that the lateral medullary vein (arrow in (b)) drains into the SCS (double arrows in (a) and (b)) via a SCS BV (arrowhead). Star shows the right vertebral artery

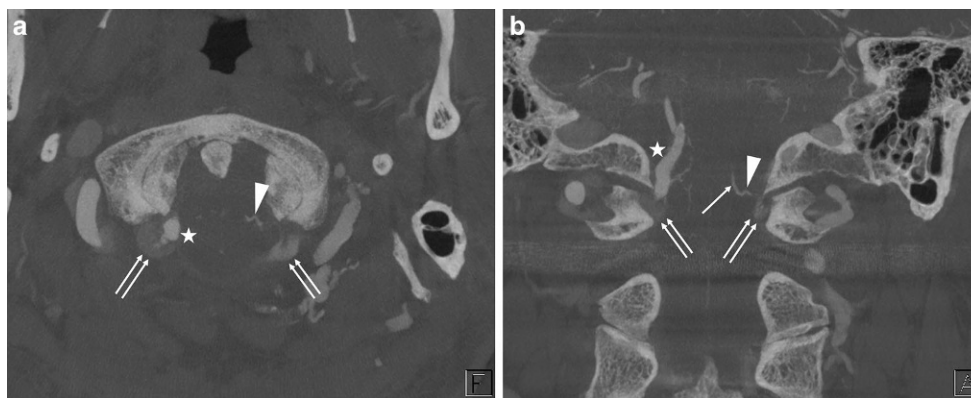


Fig. 7 A representative case of the cerebellomedullary cistern (CMC) bridging vein (BV). Axial (a) and sagittal (b) view of the slab MIP images from contrast-enhanced cone-beam CT show that the transverse medullary vein (arrow in (a)) and posterior spinal vein (arrow in (b)) drain into the marginal sinus (double arrows in (a) and (b)) via a CMC BV (arrowhead), which is the posteromedian BV running through the CMC. Star shows the right vertebral artery



Table 1 Detection rate of each bridging vein around the foramen magnum

	Ipsilateral to VAG (%)	Contralateral to VAG (%)	Any side (%)
ACV BV	4 (7)	8 (14)	11 (19)
JF BV	15 (26)	7 (12)	18 (32)
MS BV	23 (40)	16 (28)	32 (56)
SCS BV	13 (23)	10 (18)	20 (35)
CMC BV	–	–	16 (28)
All BVs	–	–	55 (96)

ACV anterior condylar vein; BV bridging vein; CMC cerebellomedullary cistern; JF jugular foramen; MS marginal sinus; SCS suboccipital cavernous sinus; VAG vertebral angiography

1. The ACV BV empties into the ACV (Fig. 3).
2. The jugular foramen (JF) BV empties into the inferior petrosal sinus, sigmoid sinus, or jugular bulb (Fig. 4).
3. The MS BV empties into the MS other than the posteromedian direction (Fig. 5).
4. The SCS BV empties into the SCS (Fig. 6).
5. The cerebellomedullary cistern (CMC) BV is a posteromedian BV emptying into the MS or occipital sinus (Fig. 7).

Based on our classification of BVs around the FM, among the total of 122 BVs, 12 BVs were ACV BV, 24 were JF BV, 45 were MS BV, 25 were SCS BV, and 16 were CMC BV.

Detection Rate and Diameter of Each BV

Among the 57 patients, we calculated the detection rate of each BV divided into the ipsilateral and contralateral side to VA angiography except for the CMC BV located midline (Table 1). On the ipsilateral side of VA angiography, ACV, JF, MS, and SCS BVs were detected in 4 (7%), 15 (26%), 23 (40%), and 13 patients (23%), respectively. On the contralateral side of VA angiography, ACV, JF, MS, and SCS BVs were detected in 8 (14%), 7 (12%), 16 (28%), and 10 patients (18%), respectively. On any side, ACV, JF, MS, and SCS BVs were detected in 11 (19%), 18 (32%), 32 (56%), and 20 patients (35%), respectively. The CMC BV was detected in 16 patients (28%). Any BV was detected on any side in 55 patients (96%). There were 10 cases (MS, 6; JF, 2; SCS, 2) with two same-subtype BVs on the same side. The mean diameters (range) of ACV, JF, MS, SCS, and CMC BVs were 0.6 (0.4–0.9) mm, 0.6 (0.3–0.9) mm, 0.6 (0.3–1.2) mm, 0.6 (0.3–0.9) mm, and 0.8 (0.5–1.3) mm, respectively.

Discussion

In the present study, we demonstrated that a total of 122 BVs were detected (median, 2 per patient) and that 55 patients (96%) had any BVs around the FM. We classified the BVs into five subtypes based on the draining pattern. The MS BV was the most frequent, and the CMC BV was the largest.

Historically, supratentorial and cerebellar BVs have been systematically investigated in cadaveric and radiological studies [1, 2]. Rhoton divided the BVs of the posterior fossa into four groups: the galenic group draining into the vein of Galen; the tentorial group draining into the torcular and tentorial sinus; the petrosal group draining into the petrosal sinus; and other BVs [4]. In this article, some BVs around the FM have been listed as one of the “other” infrequent BVs. Baltasvias et al. summarized medullary BVs in their review article [5]. Although they described BVs draining into the inferior petrosal sinus, sigmoid sinus, jugular bulb, MS, ACV, and occipital sinus, the description was not carried out in a systematic manner.

Duvernoy reported detailed venous anatomy around the brainstem based on 50 cadaver brains [6]. He mainly described the BVs as the “satellite veins of the cranial nerves,” not as BVs. He demonstrated the satellite veins running alongside the ninth to twelfth cranial nerves and the first cervical nerve root in figures. The satellite veins of the glossopharyngeal and vagal nerve drained into the inferior petrosal sinus around the JF and were called the inferior petrosal vein. These veins may represent the JF BV in the present study. Similarly, the satellite vein of the hypoglossal nerve is thought to be the ACV BV, and the satellite vein of the first cervical nerve root could be the SCS BV. Duvernoy reported that the frequency of the satellite veins described as the glossopharyngeal nerve, hypoglossal nerve, and first cervical nerve root was 30, 8, and 32%, respectively.

Duvernoy also reported the vein of the cerebellomedullary cistern. The posteromedian medullary vein drains downward into the MS through the vein of the cerebellomedullary cistern, which is the same vein as our CMC BV. He reported that the frequency of this vein was 50%. Matsushima also reported detailed venous anatomy of the BVs based on 25 cadaver brains [7]. The BVs drained into the in-

ferior petrosal sinus near the JF, and the inferior part of the sigmoid sinus appeared in 8.3 and 37.5% cadavers. We assume that the JF BV in the present study represents these veins by Matsushima. Matsushima also demonstrated that another BV that drained into the MS around the FM appeared in 41.7% of cadavers, which may represent the MS BV. Kiyosue et al. reported the anterior medullary-anterior pontomesencephalic venous system and its BVs based on gadolinium-enhanced MRI in 35 patients [8]. They identified BVs connecting to the SCS in 11 cases (31%), inferior petrosal sinus in 5 cases (14%), MS in 3 cases (9%), and jugular bulb in 1 case.

In the spinal region, there are two kinds of drainage veins from the spinal cord: radiculomedullary veins and BVs. The radiculomedullary veins run along the nerve root and pierce the dura at the spinal nerve root sleeve. The BVs of the spinal cord run apart from the nerve root and pierce the dura independently of the nerve root sleeve. We believe that the satellite veins described by Duvernoy [7] correspond to the radiculomedullary veins; hence, some ACV, JF, and SCS BVs are radiculomedullary veins. However, the MS and CMC BVs correspond to the BVs of the spinal cord because they run apart from the cranial nerve root. It was challenging to differentiate between radiculomedullary veins and BVs because there are no data regarding the nerve root in the collected data in the present study. Therefore, we defined the BVs as including the radiculomedullary veins in this study.

We summarized the frequency of each BV in the published literature and our results in Table 2. In the present study, the frequency of each BV is higher than in the MRI study. This difference is due to the use of images with higher spatial resolution, which increases the detection rate and makes it comparable to cadaver studies. As shown in Table 2, the published literature has only partially demonstrated the frequency of BVs, but we can systematically assess the frequency in the present study. Moreover, the current research has the largest number of study subjects.

Clinical Implications

BVs around the FM may be involved in dAVF as draining veins. Mitsuhashi et al. reported dAVFs draining into the

Table 2 Summary of reported detection rate of bridging veins around the foramen magnum

Author	Method	Number	ACV BV (in %)	JF BV (in %)	MS BV (in %)	SCS BV (in %)	CMC BV (in %)
Duvernoy	Cadaver	50	8	>30	<i>n. d.</i>	32	50
Matsushima	Cadaver	25	<i>n. d.</i>	45.8	41.7	<i>n. d.</i>	<i>n. d.</i>
Kiyosue	Gd-MRI	35	<i>n. d.</i>	17	9	31	<i>n. d.</i>
Present study	3D-RA CBCT	57	19	32	56	35	28

ACV anterior condylar vein; BV bridging vein; CBCT cone-beam CT; CMC cerebellomedullary cistern; Gd Gadolinium; JF jugular foramen; MS marginal sinus; SCS suboccipital cavernous sinus; 3D-RA 3D rotational angiography

petrosal vein or BV of the medulla [3]. They described six patients with dAVF draining into the BVs of the medulla, and all of them were dAVFs of the FM or craniocervical junction (CCJ). They also described these dAVFs as having male predominance and a higher incidence of aggressive neurological manifestations than dAVFs of the transverse-sigmoid or cavernous sinus. Recently, angioarchitecture and characteristics of CCJ and FM dAVF have been analyzed in detail [9, 10]. Most CCJ and FM dAVF involve the BVs around the FM. Based on the anatomical location, the CCJ dAVF in the occipital-C1 level may involve the SCS BV, and the FM dAVF may involve the other types of BVs. Spittau et al. reviewed the dAVFs of the hypoglossal canal. They classified them into three types in terms of their dominant venous drainage: Type 1, antegrade; Type 2, retrograde orbital; Type 3, pial or perimedullary [11]. The dAVF of the hypoglossal canal with perimedullary drainage may involve the ACV BV. Kawasaki et al. showed a hypoglossal canal dAVF with venous reflux to the medulla oblongata via the ACV BV using slab MIP images [12]. Byun et al. reported a case of JF dAVF with venous reflux to the brainstem via the BV, which was assumed to be JF BV [13]. Sugiura et al. reported sigmoid sinus dAVF with venous reflux to the medulla oblongata via the JF BV [14]. Tanaka et al. reported the occipital sinus dAVF with venous reflux to the medulla oblongata via the CMC BV [15]. Knowledge of these BVs helps us understand angioarchitecture in these complicated dAVF around the FM.

Study Limitations

There were some study limitations. First, we could not clearly identify the dural sinus to which the BVs connect in some cases. Second, due to the perfusion area of the VA, the contralateral side is not sufficiently opacified with contrast media for evaluation in some cases. Although CT angiography or enhanced MRI can solve these problems, the present study has the advantage of angiographic images of the dominant side VA with higher spatial resolution, which increases the detection rate.

Conclusions

FM BVs are frequently observed. Because of the rich surrounding venous network, they drain in various terminations.

Acknowledgements We express our heartfelt thanks to the collaborating doctors who devoted their time to this investigation: Hisayuki HOSOO, Department of Neurosurgery, Tsukuba University, Tsukuba; Yasushi MATSUMOTO, Department of Neurosurgery, Tohoku University, Sendai; Takeo NISHIDA, Department of Neurosurgery, Osaka University; Naoki AKIOKA, Department of Neurosurgery, Toyama University, Toyama; Akira ISHII and Masakazu OKAWA, Department

of Neurosurgery, Kyoto University, Kyoto; Wataro TSURUTA, Department of Endovascular Neurosurgery, Toranomon Hospital, Tokyo, Japan.

Funding Open access funding provided by Okayama University.

Declarations

Conflict of interest M. Hiramatsu, T. Ozaki, S. Tanoue, K. Mizutani, H. Nakamura, K. Tokuyama, H. Sakata, Y. Matsumaru, I. Nakahara, Y. Niimi, T. Fujinaka and H. Kiyosue declare that they have no competing interests.

Ethical standards All procedures performed in studies involving human participants were performed in accordance with the ethical standards of our institutional research committee. The institutional review boards approved this retrospective study in all collaborative institutions. Written informed consent was obtained from all patients before angiography.

Open Access This article is licensed under a Creative Commons Attribution 4.0 International License, which permits use, sharing, adaptation, distribution and reproduction in any medium or format, as long as you give appropriate credit to the original author(s) and the source, provide a link to the Creative Commons licence, and indicate if changes were made. The images or other third party material in this article are included in the article's Creative Commons licence, unless indicated otherwise in a credit line to the material. If material is not included in the article's Creative Commons licence and your intended use is not permitted by statutory regulation or exceeds the permitted use, you will need to obtain permission directly from the copyright holder. To view a copy of this licence, visit <http://creativecommons.org/licenses/by/4.0/>.

References

1. Brockmann C, Kunze S, Scharf J. Computed tomographic angiography of the superior sagittal sinus and bridging veins. *Surg Radiol Anat.* 2011;33:129–34. <https://doi.org/10.1007/s00276-010-0714-5>.
2. Han H, Yao Z, Wang H, Deng X, Deng X, Yu Fong AH, Zhang M. Dural entrance of the bridging vein into the transverse sinus provides a reliable measure for preoperative planning: an anatomic comparison between cadavers and neuroimages. *Neurosurgery.* 2008;62(5 Suppl 2):ONS289–95. <https://doi.org/10.1227/01.neu.0000326009.46197.ab>.
3. Mitsushashi Y, Aurboonyawat T, Pereira VM, Geibprasert S, Toulgoat F, Ozanne A, Lasjaunias P. Dural arteriovenous fistulas draining into the petrosal vein or bridging vein of the medulla: possible homologs of spinal dural arteriovenous fistulas. *J Neurosurg.* 2009;111:889–99. <https://doi.org/10.3171/2009.1.JNS08840>.
4. Rhoton AL Jr. The posterior fossa veins. *Neurosurgery.* 2000;47(3 Suppl):S69–S92. <https://doi.org/10.1097/00006123-200009001-00012>.
5. Baltasvias G, Parthasarathi V, Aydin E, Al Schameri RA, Roth P, Valavanis A. Cranial dural arteriovenous shunts. Part 1. Anatomy and embryology of the bridging and emissary veins. *Neurosurg Rev.* 2015;38:253–63. <https://doi.org/10.1007/s10143-014-0590-2>. discussion 263–4.
6. Duvernoy HM. The superficial veins of the human brain: veins of the brain stem and of the base of the brain. Berlin: Springer; 1975.
7. Matsushima T, Rhoton AL Jr, de Oliveira E, Peace D. Microsurgical anatomy of the veins of the posterior fossa. *J Neurosurg.* 1983;59:63–105. <https://doi.org/10.3171/jns.1983.59.1.0063>.

8. Kiyosue H, Tanoue S, Sagara Y, Hori Y, Okahara M, Kashiwagi J, Nagatomi H, Mori H. The anterior medullary-anterior pontomesencephalic venous system and its bridging veins communicating to the dural sinuses: normal anatomy and drainage routes from dural arteriovenous fistulas. *Neuroradiology*. 2008;50:1013–23. <https://doi.org/10.1007/s00234-008-0433-3>.
9. Hiramatsu M, Sugiu K, Ishiguro T, Kiyosue H, Sato K, Takai K, Niimi Y, Matsumaru Y. Angioarchitecture of arteriovenous fistulas at the craniocervical junction: a multicenter cohort study of 54 patients. *J Neurosurg*. 2018;128:1839–49. <https://doi.org/10.3171/2017.3.JNS163048>.
10. Yoo DH, Cho YD, Boonchai T, Kim KM, Kim JE, Cho WS, Lee SH, Chung CK, Kang HS. Endovascular treatment of medullary bridging vein-draining dural arteriovenous fistulas: foramen magnum vs. craniocervical junction lesions. *Neuroradiology*. 2022;64:333–42. <https://doi.org/10.1007/s00234-021-02790-z>.
11. Spittau B, Millán DS, El-Sherifi S, Hader C, Singh TP, Motschall E, Vach W, Urbach H, Meckel S. Dural arteriovenous fistulas of the hypoglossal canal: systematic review on imaging anatomy, clinical findings, and endovascular management. *J Neurosurg*. 2015;122:883–903. <https://doi.org/10.3171/2014.10.JNS14377>.
12. Kawasaki Y, Kanamori F, Tsukada T, Shintai K, Takasu S, Seki Y. Surgical disconnection of a hypoglossal canal dural arteriovenous fistula demonstrating rapid progression of medulla oblongata disturbance: illustrative case. *J Neurosurg Case Lessons*. 2022;3:CASE21657. <https://doi.org/10.3171/CASE21657>.
13. Byun JS, Hwang SN, Park SW, Nam TK. Dural arteriovenous fistula of jugular foramen with subarachnoid hemorrhage: selective transarterial embolization. *J Korean Neurosurg Soc*. 2009;45:199–202. <https://doi.org/10.3340/jkns.2009.45.3.199>.
14. Sugiura Y, Nozaki T, Sato H, Sawashita K, Hiramatsu H, Nishizawa S. Sigmoid sinus dural arteriovenous fistula with spinal venous drainage manifesting as only brainstem-related neurological deficits without myelopathy: case report. *Neurol Med Chir*. 2009;49:71–6. <https://doi.org/10.2176/nmc.49.71>.
15. Tanaka J, Fujita A, Maeyama M, Kohta M, Hosoda K, Kohmura E. Cognard type V dural arteriovenous fistula involving the occipital sinus. *J Stroke Cerebrovasc Dis*. 2017;26:e62–e3. <https://doi.org/10.1016/j.jstrokecerebrovasdis.2017.01.004>.